Supplemental Information

Androgen receptor functions as transcriptional repressor of Cancer Associated Fibroblast activation

Andrea Clocchiatti[1,2*], Soumitra Ghosh[3*], Maria-Giuseppina Procopio[3], Luigi Mazzeo[3], Pino Bordignon[3], Paola Ostano[4], Sandro Goruppi[1,2], Giulia Bottoni[1], Atul Katarkar[3], Mitchell Levesque[5], Peter Kölblinger[5,6], Reinhard Dummer[5], Victor Neel[7], Berna C. Özdemir[8,9] and G. Paolo Dotto[1,3,9+]

[1]Cutaneous Biology Research Center, Massachusetts General Hospital, Charlestown, MA 02129, USA

[2] Department of Dermatology, Harvard Medical School, Boston, MA 02125, USA

[3]Department of Biochemistry, University of Lausanne, Epalinges 1066, Switzerland

[4]Cancer Genomics Laboratory, Edo and Elvo Tempia Valenta Foundation, Biella 13900, Italy.

[5]Department of Dermatology, University Hospital Zürich, Zürich CH-8091, Switzerland

[6]Department of Dermatology, Paracelsus Medical University, Salzburg, Austria

[7]Department of Dermatology, Massachusetts General Hospital, Boston, MA 02114, USA.

[8]Department of Oncology, Centre Hospitalier Universitaire Vaudois, 1011 Lausanne, Switzerland

[9]International Cancer Prevention Institute, Epalinges 1066, Switzerland

* equally contributed to this work

[+] to whom correspondence should be addressed : paolo.dotto@unil.ch

Key words: androgen receptor, Notch/CSL, cancer associated fibroblasts, skin SCC, melanoma

Running Title: Androgen receptor suppresses CAF activation

SUPPLEMENTAL METHODS

Isolation of HDFs and CAFs

Derivation of HDF and CAFs was performed as in (33). Briefly, surgically excised discarded skin SCCs samples, or non-affected skin samples, were cut into 1–2 mm pieces after removal of excess fat, followed by incubation in 2 ml of PBS containing 0.25 mg/ml of Liberase TL (Roche) for 40 min at 37 °C with gentle shaking. After equal volume addition of fetal bovine serum to stop the enzymatic digestion, the dissociated tissue was passed through a 10 ml syringe attached to a 70µm sieve. Cells from the flow through were centrifuged, washed three times with DMEM 10% fetal bovine serum and seeded in 10 cm tissue culture dishes. Adherent cells were expanded for characterization as with HDFs. In some cases we derived simultaneously matched normal HDFs from the same patient using discarded non-diseased area Each HDF and CAF strain was given specific and progressive letter/number identification as indicated in the different panels. The identifier of the operator and a progressive number classify each primary HDF strain (e.g. HDF AC3) and a list of all the cells used is provided in Supplemental Table 4 and 5.

Immunofluorescence

The frozen tissue sections or cultured cells on glass coverslips were fixed with cold 4% paraformaldehyde (PFA) for 15 minutes at room temperature (RT). The fixed cells were washed with PBS followed by permeabilization with 0.1%

TritonX100 in PBS for 10 minutes and incubated with 2% bovine serum albumin in PBS for 2 hours at RT. Primary antibodies were diluted in fluorescence dilution buffer, 2% bovine serum albumin in PBS, pH 7.6 and incubated over night at 4°C. After washing 3 times in PBS the samples were incubated with donkey fluorescence conjugated secondary antibodies (Invitrogen) for 1 hour at RT. After washing with PBS the slides were mounted with Fluoromount Mounting Medium (Sigma-Aldrich) after nuclear DAPI staining. Immunofluorescence images were acquired with a ZEISS LSM510 or ZEISS LSM880 confocal microscope with 20X or 40X oil immersion objectives. We used NIS Elements software for the acquisition and processing of the images. For fluorescence signal quantification, acquired images for each color channel were imported into either Adobe Photoshop software, followed by Lasso Tool selection, or ImageJ software, using the functions “measurement” or “particle analysis” for selection of areas or cells (tumor or stromal) of interest. All measurements were exported as Microsoft Excel data files. A detailed list of all the antibodies used is in Supplemental Table 3.

Cell based assays

Senescence β-galactosidase (SA-β-Gal) activity assays was assessed by use of a commercially available chromogenic assay kit (Cell Signalling). For cell growth assays cell were plated at a density of 4×10^4 in 1 ml of medium. At the indicated time points cells were detached using trypsin for 5 minutes at 37°C, centrifuged and the pellet was re-suspended in 200 μl of medium for counting using

Neubauer chamber. Cells were replenished with fresh medium every two days. For SK-MEL-23 time course studies cells were seeded at a density of 4 x 10^4 in 1 ml of medium. The following day cells were treated with 100 nM Jq1 (Adooq Biosciences) or DMSO. At the indicated time points cells were detached using trypsin for 5 minutes at 37°C, centrifuged and the pellet was re-suspended in 200 µl of medium for counting using Neubauer chamber. Cells were replenished with fresh medium plus/minus drug treatment after 48h. EDU assays were performed using Click-It EDU imaging kit C10337 (Thermo Fisher Scientific) adding 10 µM EDU 3h prior fixation. Images were obtained with a Nikon Eclipse Ti confocal microscope.

Gene expression studies, Laser Capture Microdissection and RNA sequencing

Cells were lysed in Trireagent (Zymo Research) and extracted using directZol RNA miniprep kit (Zymo Research). 1 µg of total RNA was used to reverse transcribe cDNA using iScript DNA synthesis kit (Biorad) followed by real-time qPCR using the SYBR Fast qPCR master mix (Roche) in the Light Cycler 480 (Roche) according to the manufacturer's protocols. RNA samples were analyzed in triplicate with gene-specific primers using 36β4 normalization. Oligonucleotides for qPCR were designed using Primer 3 (http://bioinfo.ut.ee/primer3-0.4.0/).

SCC and flanking skin frozen samples used for LCM followed by RT-qPCR were provided by the Department of Dermatology, Massachusetts General Hospital (Boston, Massachusetts, USA), with institutional review boards approvals and

informed consent. LCM was performed using an Arcturus XT micro-dissection system (Applied Biosystems) as in (5) using β-Actin normalization. Primer sequences are indicated in Supplemental Table 3.

Total RNA was extracted 7 days after shRNA infection for AR knockdown samples using the directZol RNA miniprep kit (Zymo Research) with on-column DNase treatment. RNA quality was verified on the bioanalyzer (Agilent Technologies) with an RNA integrity number greater than 8. 1µg of total RNA was depleted of ribosomal RNA using Ribo-zero RNA removal kit (Illumina) and was used for library preparation using the Truseq kit (Illumina). A single read was done on the Illumina HiSeq 2000 sequencer at the Genomic Technologies Facility at the University of Lausanne. Reads were subjected to quality control using FastQC. Trimming was performed by means of Cutadapt (https://cutadapt.readthedocs.org/en/stable/) to find and remove adapter sequences, primers, poly-A tails. Alignment was done using STAR (https://github.com/alexdobin/STAR/releases) and reads were counted with the featureCounts tool (http://bioinf.wehi.edu.au/featureCounts/), asking for a gene-level report. DeSeq2 package (https://bioconductor.org/packages/release/bioc/html/DESeq2.html) was used to normalize count data, estimate biological variance and determine differential expression. GSEA for RNA-seq expression profiles was conducted using the software GSAA-seqSP (gene set association analysis for RNA-seq data with sample permutation from the GSAA platform (version GSAA_2.0, http://gsaa.unc.edu/) with default parameters. Curated gene sets were retrieved

from the Molecular Signatures Database (MSigDB version 5.2, http://www.broadinstitute.org/gsea/msigdb/). The pathway gene sets used in this study are listed in Supplemental Table 1. Public data sets of gene expression used for gene set enrichment analysis is GSE81406.

Proximity Ligation Assays

PLA experiments were carried out with Duolink kit (Sigma Aldrich, # DUO92101) using the following protocol. HDFs were seeded on glass overslips in a 24-well plate. After washing with PBS three times the cells were fixed with cold 4% paraformaldehyde (PFA) for 15 minutes at room temperature (RT). The fixed cells were washed with PBS followed by permeabilization with 0.1% TritonX100 in PBS for 15 minutes at RT, incubation in blocking buffer (provided with the kit) for 2 hours at 37°C in a humidified chamber, followed by incubation with primary antibodies (rabbit anti-CSL, Cell Signaling, 1: 100 and mouse anti-AR, Santa Cruz; 1:200) diluted in antibody diluents overnight at 4°C. PLA was carried out following the manufacturer's protocol. Briefly, the cells were washed in Buffer A (supplied with the kit) 3 times for 15 minutes and incubated with the PLA probes for one hour at 37°C in a humid chamber. This was followed by a 10 minutes wash in Buffer A and the ligation reaction was carried out at 37°C for one hour in a humid chamber. After washing 10 and 5 minutes in Buffer A, the cells were incubated with the amplification mix for two hours at 37°C in a darkened humidified chamber and post amplification the cells were washed with 1x Buffer

B (supplied with the kit) for 10 minutes followed by a 1 minute wash with 0.01X Buffer B and mounted using the mounting media supplied with the kit.

Immunoblot Assays

Cells were lysed in RIPA buffer (10 mM Tris-Cl (pH 8.0),1 mM EDTA,1% Triton X-100, 0.1% sodium deoxycholate,0.1% SDS, 140 mM NaCl, 1 mM PMSF) or LDS buffer (Thermo Scientific). Equal amounts of proteins were subjected to WB analysis. The membranes were sequentially probed with different antibodies as indicated in the Figure legends. The immune complex was detected by ECL kit (Thermo Scientific). The details about the antibodies used in this study are provided above in the Supplemental Table 3.

Tumorigenesis experiments

Mouse ear injections with indicated combination of cells were carried out in 8 to 10-week-old female NOD.Cg-Prkdcscid Il2rgtm1Wjl/SzJ mice (Jackson), as in (5). EGFP expressing SCC13 cells (1×10^5), EGFP expressing CAL27 cells (1×10^5), FUCCI expressing SK-MEL-23 cells (1×10^5) or SK-MEL-28 expressing dsRed (1×10^5) were admixed with equal numbers of HDFs plus/minus shRNA-mediated silencing of AR or with CAFs plus/minus AR overexpression. Cells were injected 5µl per site using a 33-gauge micro syringe (Hamilton). Mice were injected with sh CT and with sh AR HDFs as follows: for SCC13 EGFP 10 mice, for CAL27 EGFP 4, for SK-MEL-23 FUCCI 4, for SK-MEL-28 dsRed 4. Mice were sacrificed after 21 for SCC13 EGFP and CAL27 EGFP and after 27 days for SK-

MEL-23. Mice developed tumors as follows: with EGFP SCC13 9/9 for sh CTRL and 10/10 for shAR (data in Figure 7 and Supplemental Figure 4), with CAL27 EGFP 4/4 for sh CTRL and 4/4 for shAR (data in Supplemental Figure 5), with SK-MEL-23 FUCCI 4/4 for sh CTRL and 4/4 for shAR (data in Figure 8 and Supplemental Figure 6), with SK-MEL-28 dsRed 4/4 for sh CTRL and 4/4 for shAR (data in Figure 8). For tumor volume measurements one mouse has been excluded since it did not form tumor in the EGFP SCC13 sh CTRL ear. In vivo experiments using CAF derived SCC ectopically expressing LACZ or AR (1×10^5) were admixed with EGFP expressing SCC13 cells (1×10^5) and mice developed tumors as follows: with EGFP SCC13 5/5 for CAF expressing LACZ and 5/5 for CAF expressing AR (data in Figure 14 and Supplemental Figure 12); two animals developed two independent tumors. Images of ears were taken using bright field and fluorescence stereomicroscopy. For SCC13, SK-MEL-23 and SK-MEL-28 derived tumors, mouse ears were imaged using a fluorescent stereomicroscope (Leica MZ-FLIII), every three days for 21, 27 or 28 days respectively normalizing the acquired fluorescent signal on day 1. For ear injections and imaging, mice were anesthetized by intra-peritoneal injections with xylazine-ketamine solution in PBS. Mice were housed as groups and their health was monitored daily by the MGH housing facility. Experiments were run in non-blinding conditions for researchers. No adverse event was found and no modification to the experimental protocol was made. For SCC13 injection we have used 5 mice per condition to be tested, each experiment repeated twice, for a total of 10 mice using two independent human dermal fibroblasts strains. Such

number has been calculated by the predicted power of analysis using G power software. For in vivo validation experiments using SK-MEL-23, SK-MEL-28 of CAL27 cell lines we used 4 mice to minimize the number of animals.

For in vivo drug treatment mouse ear injections were set up with EGFP expressing SK-MEL-23 cells (1×10^5) admixing equal numbers CAFs. After 4 days from injection ears were treated with 20 μl of JQ1 (10 μM in Ethanol) or vehicle twice a week. For time course analysis of SK-MEL-23 derived tumors, mouse ears were imaged using a fluorescent stereomicroscope (Leica MZ-FLIII), every three days for 14 days normalizing the acquired fluorescent signal on day 1.

All animal studies were approved by the MGH/Partners institutional animal care and use committee. Immunohistochemistry of tumors was performed as in (5, 33, 47) and quantification of Ki67 protein positive cells was made using the watershed algorithm (http://imagej.nih.gov/ij/plugins/watershed.html) and ImageJ, NIH. Quantification of all other tissue immunocytochemistry staining was performed using ImageJ. Antibodies against Filaggrin and Keratin10 were purchased from Covance, Pan cytokeratin (Keratin903) from ENZO, CD68, Ki67 and Periostin were from Abcam; anti-αSMA from Sigma and anti CD31/PECAM from BD-Pharmingen; anti p53 DO1 was purchased from Santa Cruz Biotechnology. All reagents were used as indicated by manufacturer. A detailed list of all the antibodies used is in Supplemental Table 3.

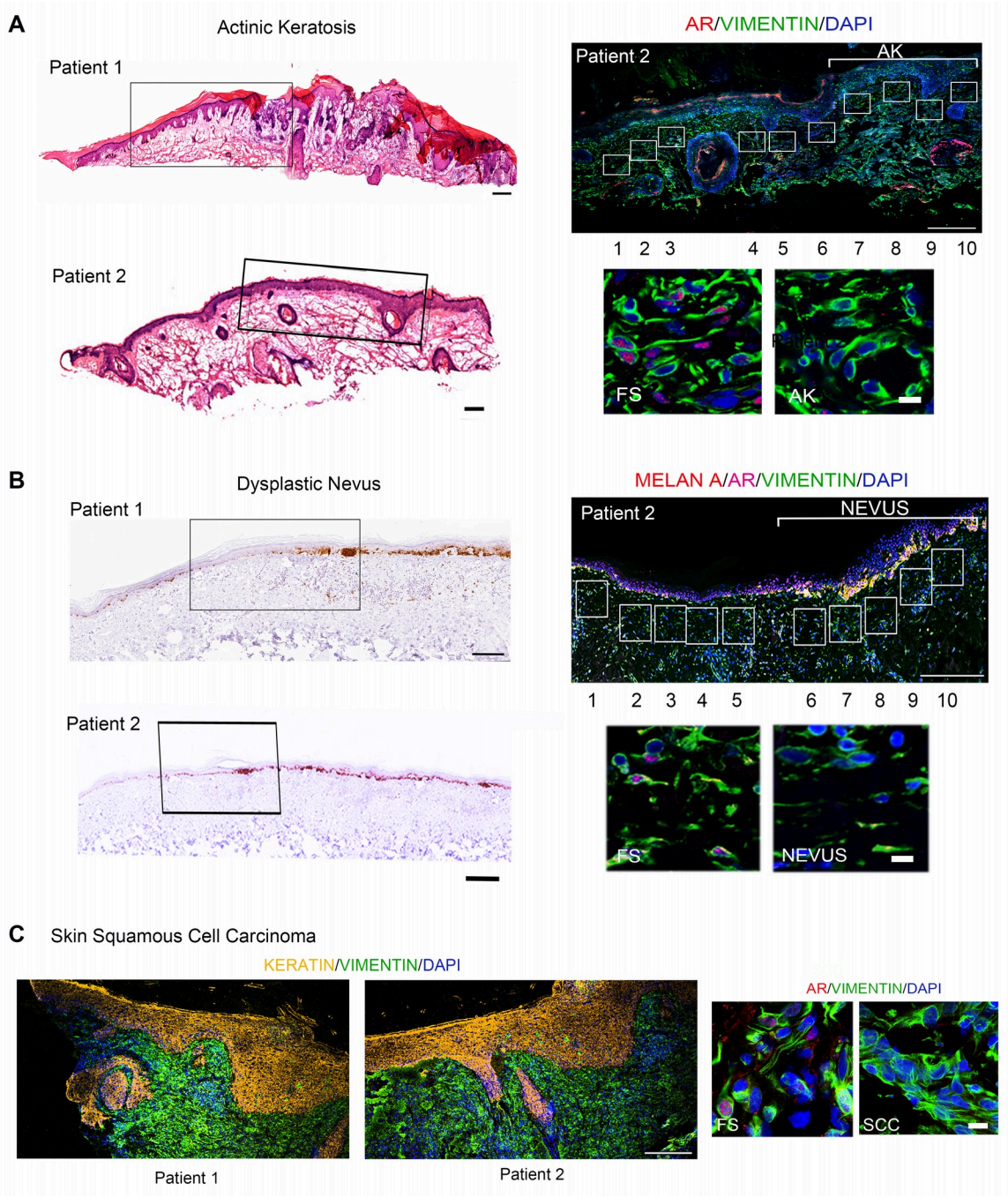

Supplemental Figure 1. Immunofluorescence staining of AR in the stromal compartment of skin cancer lesions.

(A) Left panels: low magnification hematoxylin and eosin staining of excised premalignant actinic keratosis (AK) lesions and flanking skin from two patients. Scale bar 200 μm. Right panels: IF analysis of topographically delimited stromal areas (numbered boxes) at various distance from the AK lesion from patient 2, with anti-AR (red) and anti-vimentin (green) antibodies, together with representative high magnification images used for quantification, relative to Figure 1 and Figure 2. Scale bar 200 μm (top panel) and 20 μm (bottom panel) respectively. (B) Left panels: low magnification immunohistochemical staining of premalignant dysplastic nevi (NEVUS) and flanking skin from two patients with anti-MELAN-A antibodies, for melanocytic lesion identification. Scale bar 200 μm. Right panels: IF analysis of topographically delimited stromal areas (numbered boxes) at various distance from patient 2, with anti-MELAN-A (red), anti-AR (magenta) and anti-vimentin (green) antibodies, together with representative high magnification images used for quantification, relative to Figure 1 and Figure 2. Scale bar 200 μm (top panel) and 20 μm (bottom panel) respectively. (C) Left panel: low magnification immunohistochemical staining of Squamous Cell Carcinoma lesions from two patients. Scale bar 200 μm. Right panel: representative high magnification IF images used for quantification with anti-AR (red) and anti-vimentin (green) antibodies relative to Figure 2. Scale bar 20 μm.

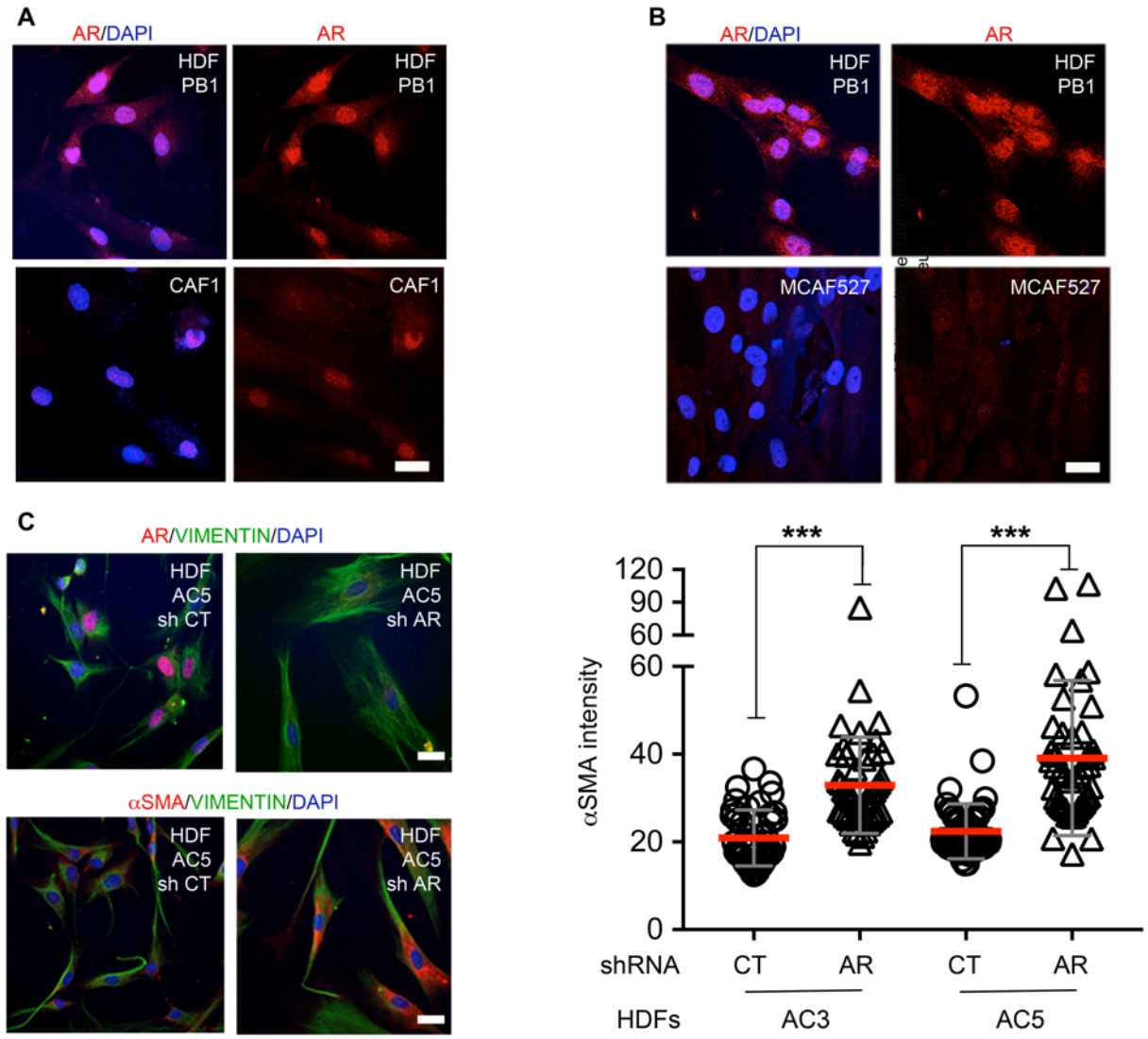

Supplemental Figure 2. AR expression is reduced in skin CAFs and its loss induces CAF activation.

(A,B) Shown are representative images of immunofluorescence analysis of AR expression in multiple CAF strains derived from skin SCC (A) or melanoma (B) as in Figure 3 versus a reference set of HDFs with anti-AR (red) antibody. Scale bar 20 µm.

(C) Double immunofluorescence analysis of AR or α-SMA (red) expression together with VIMENTIN (green) of two HDFs strains infected with an *AR* silencing lentivirus (sh AR1) versus control vector (sh CT). Shown are representative images with quantification of α-SMA signal intensity. Scale bar 60 µm. Values for each individual cell are indicated with mean ± SD. n(cell measurements per condition) = 44,***p<0.005, two-tailed paired t-test.

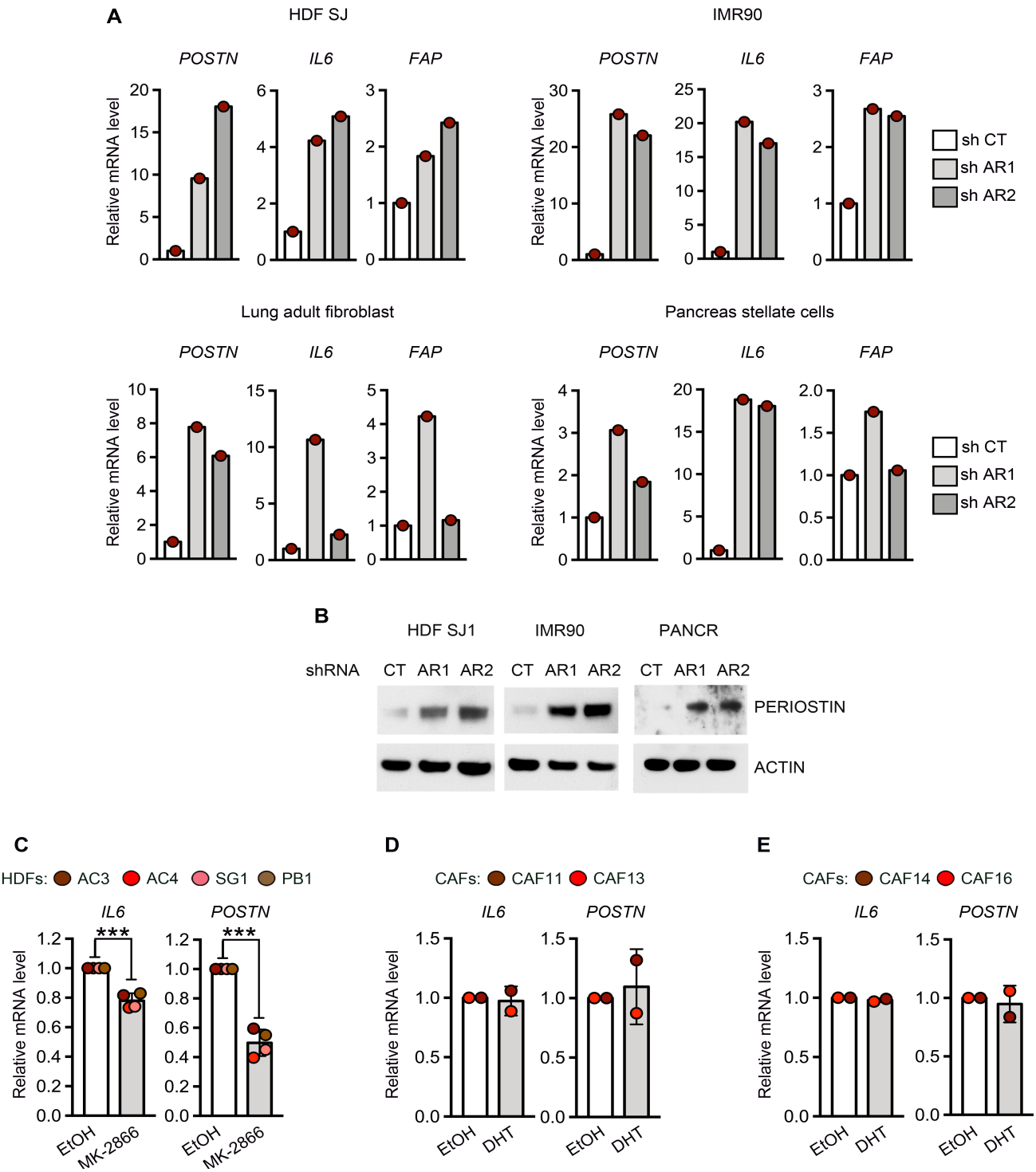

Supplemental Figure 3 AR silencing induces activation of stromal fibroblasts of different origin.
(A) RT-qPCR analysis of the indicated CAF effector genes in an additional HDF strain (SJ1, from dermis), lung IMR90 and primary (LUNG) fibroblasts and in stellate cells from pancreas (PANCR) infected with *AR* silencing lentiviruses (sh AR1, AR2) versus control vector (sh CT).
(B) Immunoblot analysis of PERIOSTIN levels in HDFs (SJ1), lung fibroblasts (IMR90) and stellate cells from pancreas (PANCR) stably infected with two different *AR* silencing lentiviruses (sh AR1, AR2) versus control vector (sh CT).
(C) RT-qPCR analysis of *IL6* and *POSTN* mRNA levels in four HDF strains treated with the AR agonist MK-2866 10 mM for 24h in parallel with ethanol (ETOH) vehicle alone. Values for each strain are indicated as dots with mean ± SD. n(HDF strains)=4,***p<0.005, two-tailed unpaired t-test.
(D,E) RT-qPCR analysis of *IL6* and *POSTN* mRNA levels in two CAF strains treated with the AR agonist dihydrotestosterone (DHT, 20 nM) for 3 days and 7 days in parallel with ethanol (ETOH) vehicle alone. Values for each strain are indicated as dots with mean ± SD.

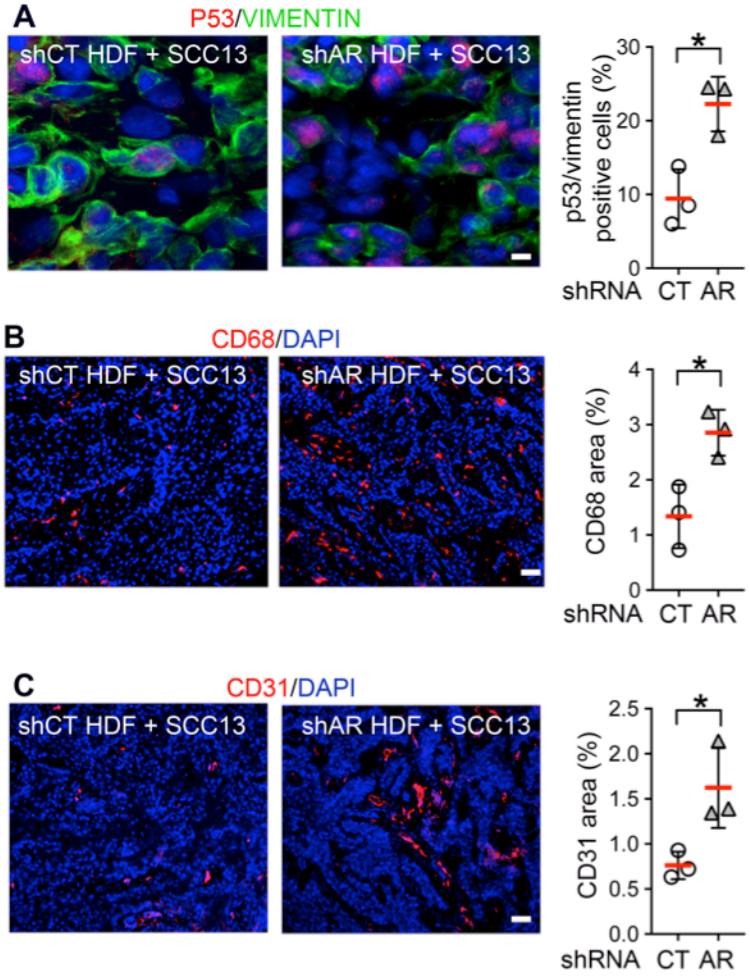

Supplemental Figure 4. HDFs with silenced *AR* enhance tumorigenicity of SCC13 cells in an orthotopic skin cancer model.

(A) Immunofluorescence analysis and quantification of p53 and VIMENTIN positive cells in lesions formed by SCC13 cells admixed with HDFs plus/minus AR silencing. Shown are representative images and quantification for 3 ear pairs, examining at least 4 independent fields per lesion. Scale bar 10μm. Data are represented as mean ± SD. n(tumor pairs) = 3, *p<0.05, two-tailed paired t test.

(B,C) Immunofluorescence analysis and quantification of the macrophage (CD68) and angiogenesis (CD31) markers in lesions formed by SCC13 cells admixed with HDFs plus/minus AR silencing. Shown are representative images and quantification for 3 ear pairs, examining at least 4 independent fields per lesion, using ImageJ software. Scale bar 60μm. Values are expressed as percentage of surface area. Data are represented as mean ± SD. n(mice) = 3, *p<0.05, two-tailed unpaired t test.

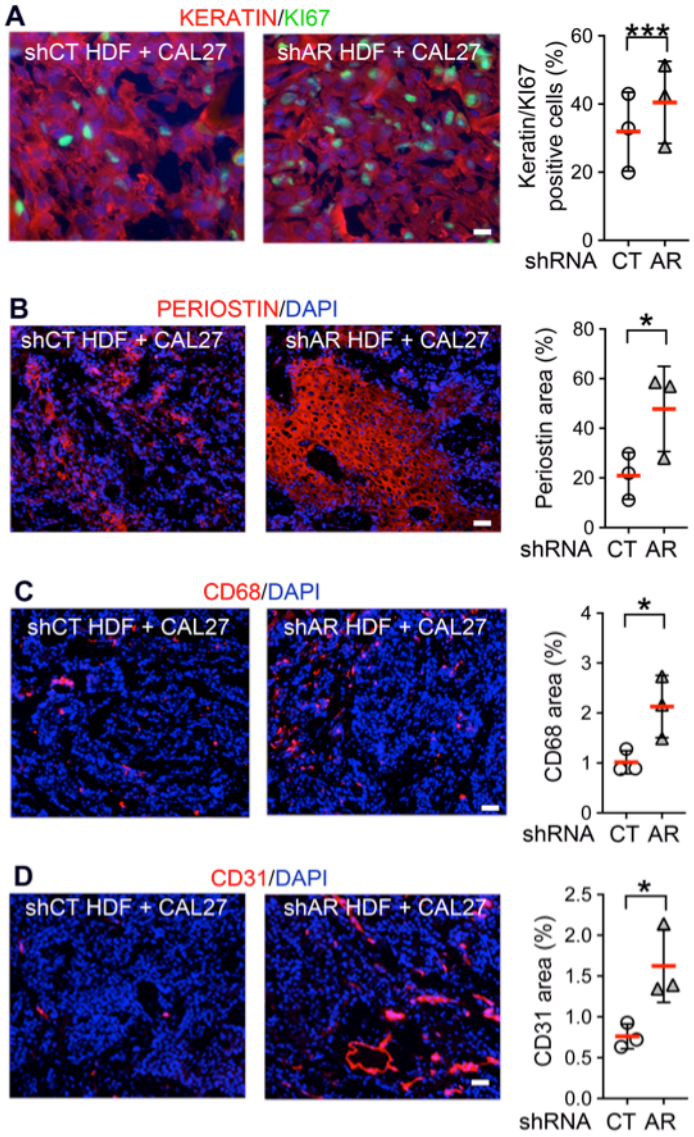

Supplemental Figure 5. HDFs with silenced *AR* enhance tumorigenicity of CAL27 SCC cells in an orthotopic skin cancer model.

(A) EGFP-expressing CAL27 SCC cells were admixed with HDFs with silenced *AR* versus control, followed by parallel injections into contralateral ears of NOD/SCID/IL2rg-/- mice (8-10 weeks old, females). Immunofluorescence analysis and quantification of KI67 and keratin positive cells in lesions formed by CAL27 cells admixed with HDFs plus/minus AR silencing. Shown are representative images and quantification for 3 ear pairs, examining at least 4 independent fields per lesion. Scale bar 30 µm. Data are represented as mean ± SD. n(tumor pairs) = 3, ***p<0.005, two-tailed paired t test.

(B-D) Immunofluorescence analysis and quantification of the indicated markers in lesions formed by CAL27 cells admixed with HDFs plus/minus AR silencing. Shown are representative images and quantification for 3 ear pairs, examining at least 4 independent fields per lesion, using ImageJ software. Values are expressed as percentage of surface area. Scale bar 60µm. Data are represented as mean ± SD. n(tumor pairs) = 3, *p<0.05, two-tailed unpaired t test.

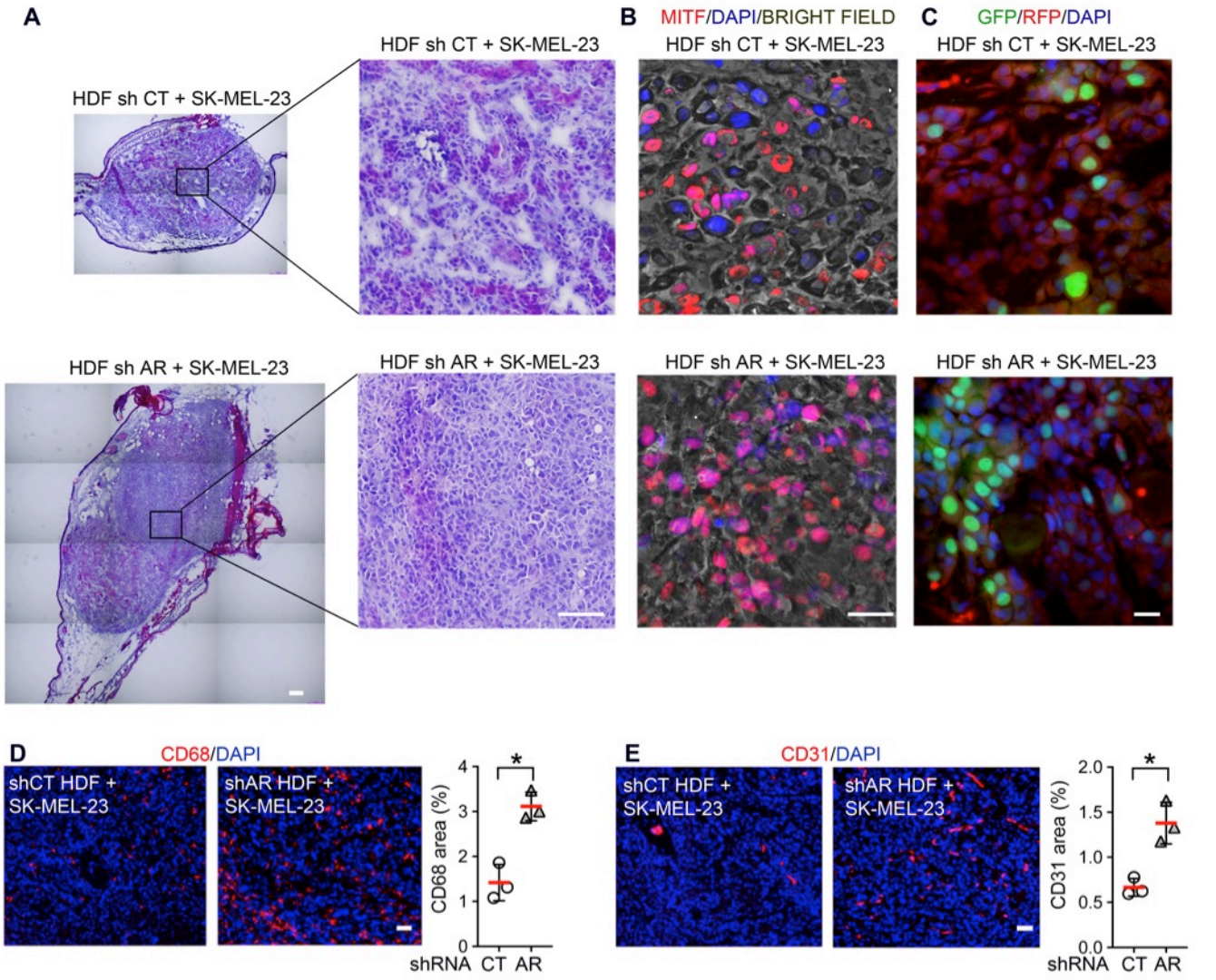

Supplemental Figure 6. HDFs with silenced *AR* promote tumorigenicity of melanoma cells in an orthotopic skin cancer model.

(A) Haematoxylin and eosin staining of tumors formed by SK-MEL-23 admixed with HDFs with silenced *AR* versus control. Scale bar : 200 and 60 μm for left and right panels, respectively.

(B) Overlaid bright field and immunofluorescence images of lesions formed by SK-MEL-23 cells admixed with HDFs plus/minus AR silencing stained for MITF (red) and DAPI (blue). Scale bar : 20 μm.

(C) Analysis of lesions formed by SK-MEL-23 cells expressing the lentivirally transduced indicators of the S/G2 (GFP) and G1 (RFP) phases of the cell cycle in the presence of HDFs plus/minus *AR* silencing. GFP and RFP exhibited nuclear versus cytoplasmic localization, respectively. Approximately two folds difference of nuclear GFP positive melanoma cells was found in lesions formed in the presence of HDFs plus/minus *AR* silencing (27% vs 14%, scoring at least 800 cells in 5 fields per lesion). Scale bar 20 μm.

(D,E) Immunofluorescence analysis and quantification of macrophage (CD68) and endothelial (CD31) markers in lesions formed by SK-MEL-23 cells admixed with HDFs plus/minus AR silencing. Representative images and quantification for 3 tumor pairs, examining at least 4 independent fields per lesion, using ImageJ software. Scale bar 60μm. Values are expressed as percentage of surface area. Data are represented as mean ± SD. n(tumor pairs) = 3, *p<0.05, two-tailed unpaired t test.

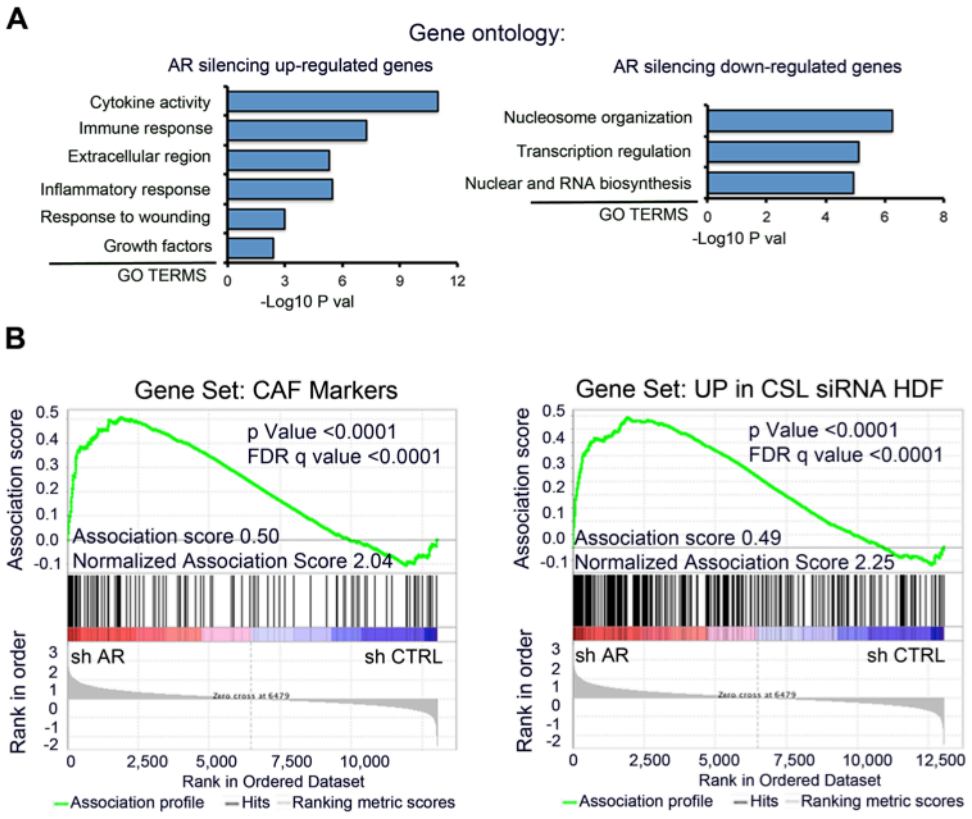

Supplemental Figure 7. *AR* silencing induces a CAF-like gene expression profile.
(A) Gene Ontology analysis of RNA-seq profiles from two HDF strains plus/minus *AR* gene silencing by infection with two different shRNA lentiviral vectors versus control. Shown are families of most significantly up- and down-regulated genes by DAVID v6.8; p-values: Fisher's exact test. For a complete list see Supplemental Table 1.
(B) Plot for gene set enrichment analysis (GSEA) using RNA-seq expression profiles of two HDF strains with *AR* gene silencing versus control against the gene expression signatures of up-regulated genes in HDFs with silenced *CSL* (5) (right panel) and of 165 genes bearing on various aspects of CAF activation (6) (left panel). Genes are ranked by signal-to-noise ratio based on their differential expression in *AR*-silenced versus control HDFs; position of genes in the *CSL* and CAF gene sets is indicated by black vertical bars, and the enrichment score is shown in green.

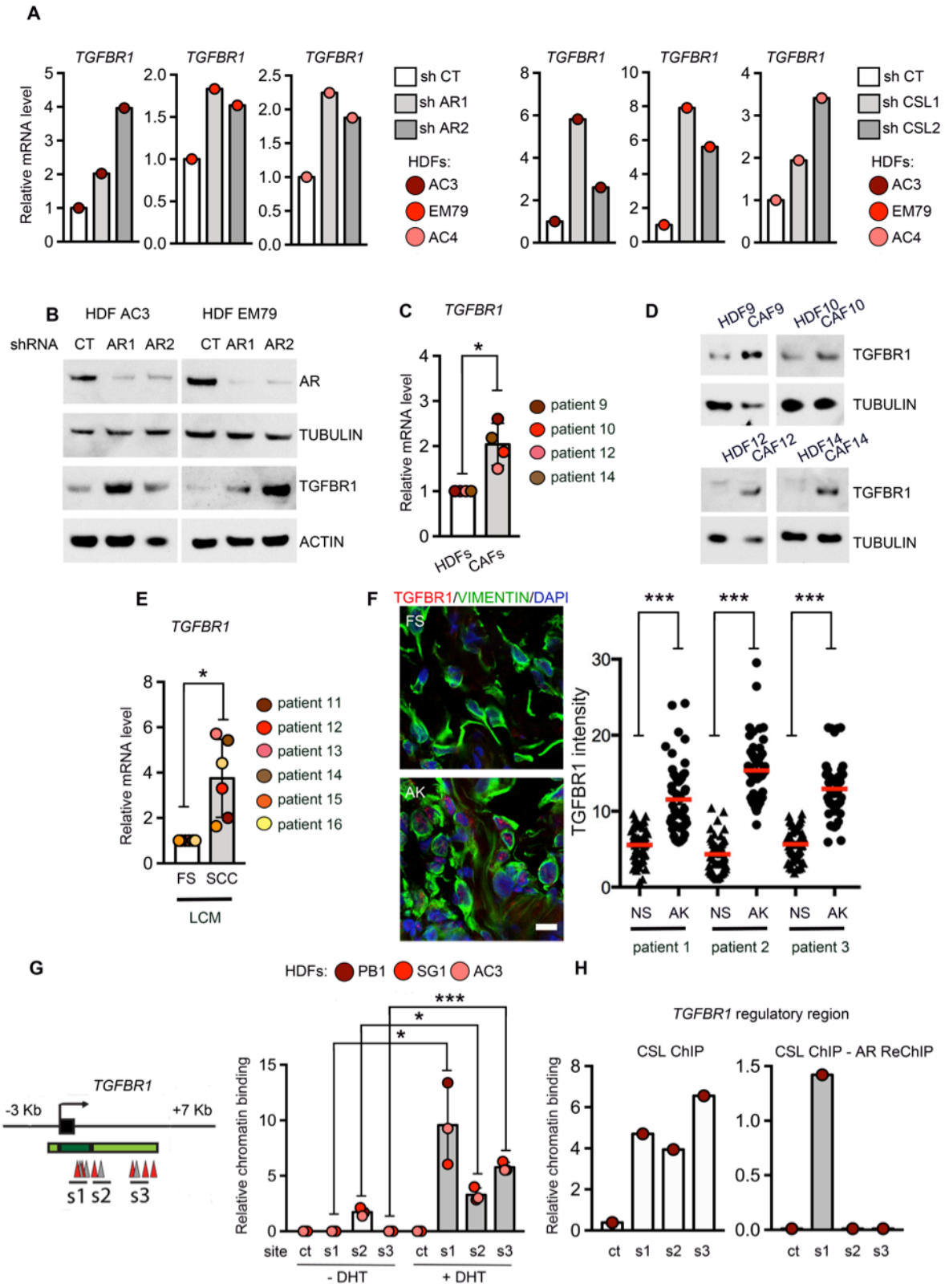

Supplemental Figure 8. *AR* and *CSL* silencing in HDFs induce TGFBR1 expression.
(A) RT-qPCR analysis of *TGFBR1* expression in HDF strains infected with *AR* (left) or *CSL* (right) silencing lentiviruses. n(HDF strains)=3.
(B) Immunoblot analysis of TGFBR1 levels in two HDF strains plus/minus *AR* silencing lentiviruses.
(C,D) RT-qPCR analysis (C) and immunoblot analysis (D) of *TGFBR1* expression in SCCs CAF strains versus matched HDFs from flanking skin. Values for each strain are indicated as dots with mean ± SD. n(HDF and CAF strains)=4,*p<0.05, two-tailed unpaired t-test.

(E) Fluorescence-guided laser capture microdissection (LCM) of fibroblasts (PDGFRα-positive cells) from SCC stroma versus flanking skin followed by RT–qPCR analysis of *TGFBR1* expression. Values for each patient are indicated as dots with mean ± SD. n(patients)=6, two-tailed paired *t*-test *p<0.005.

(F) Immunofluorescence TGFBR1 fluorescence signal quantification of AK stromal areas compared to flanking skin (FS) with anti-TGFBR1 (red) and anti-VIMENTIN (green) antibodies. Scale bar 10 μm. Values for each individual cells indicated with mean ± SD. n (cells per lesion or matched skin) =35, ***p<0.005, two-tailed paired t-test.

(G) Left panel: Map of the predicted AR and CSL binding sites (gray and red arrowheads, respectively) on the indicated region of the *TGFBR1* gene encompassing promoter and downstream enhancer. Right panel: ChIP assays of three different HDF strains with an anti-AR antibodies versus non-immune IgGs and values for each strain are indicated as dots with mean ± SD. n(HDF strains)=3, ***p<0.005, *p<0.05, two-tailed unpaired t-test.

(H) ChIP and re-ChIP assays based on immunoprecipitation with anti-CSL antibodies alone or sequentially with anti-AR antibodies (left and right panels respectively). Data are expressed as relative fold of enrichment over IgGs.

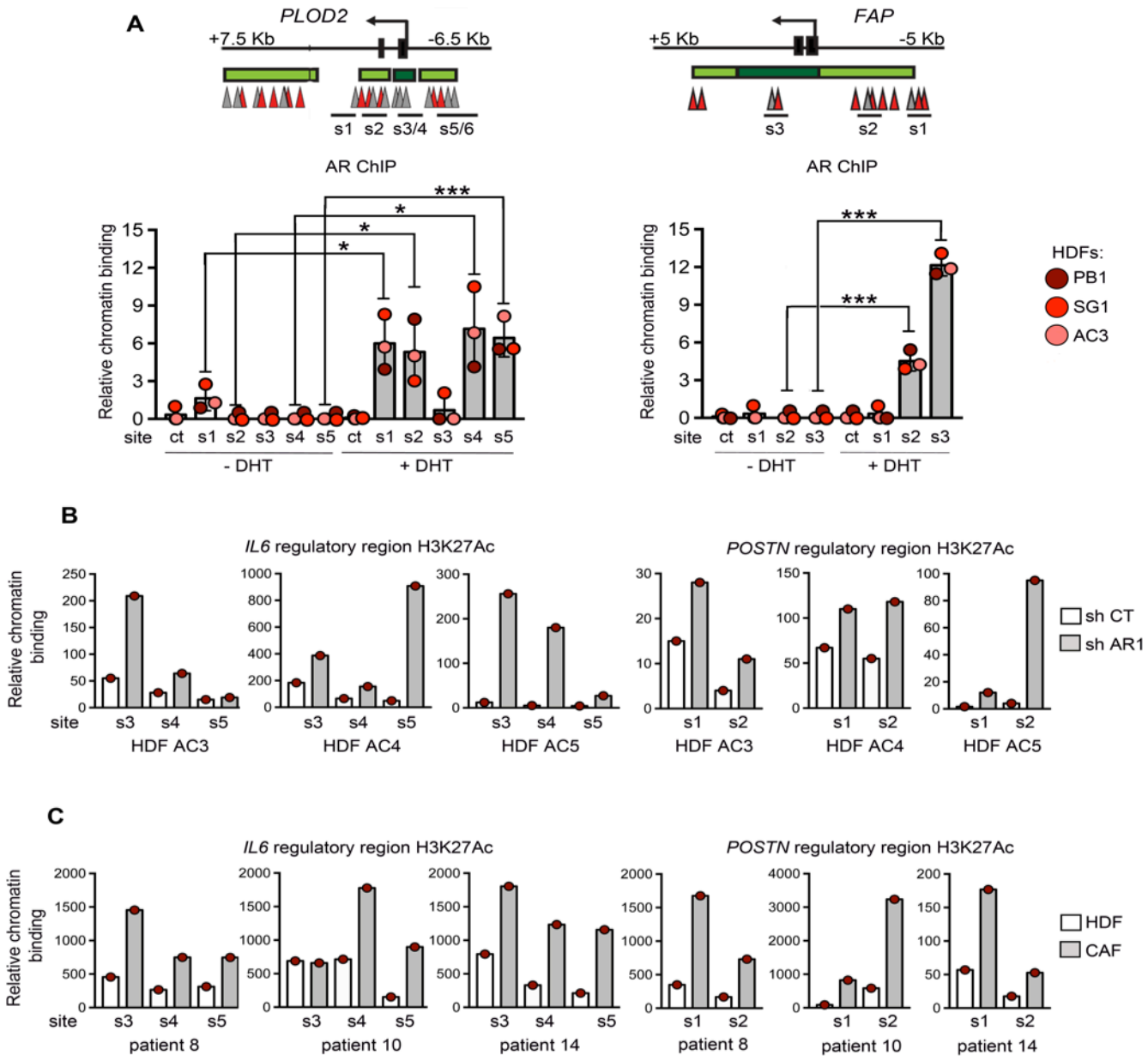

Supplemental Figure 9. AR binds the regulatory region of CAF genes controlling H3K27 Acetylation levels.

(A) Upper panel: map of predicted AR and CSL binding sites (gray and red arrowheads, respectively) on selected regions of the *PLOD2* and *FAP* genes encompassing promoter and flanking enhancer regions. Lower panel: ChIP assays of three HDF strains with anti-AR antibodies versus non-immune IgGs in absence or presence of dihydrotestosterone (DHT, 10 nM, 24h) for the indicated sites of the *PLOD2* and *FAP* genes with AR consensus sequences together with a flanking region devoid of such sequences (ct). Data are expressed as relative folds enrichment over IgGs. Statistical significance was calculated between AR enrichment at the indicated sites relative to the flanking control region. n(HDF strains)=3, ***p<0.005, *p<0.05, two-tailed unpaired t-test.

(B) ChIP assays with anti-H3K27Ac antibodies of the AR binding promoter region of the *IL6* and *POSTN* genes (left and right panels, respectively) in three independent HDF strains plus/minus *AR* silencing. Data are expressed as relative fold of enrichment over IgGs. Values for each strain are indicated as dots with mean ± SD. n(HDF strains)=3.

(C) ChIP assays with anti-H3K27Ac antibodies of the AR binding promoter region of the *IL6* and *POSTN* genes (left and right panels, respectively) in three SCC-derived CAF strains versus matched HDFs from flanking skin. Data are expressed as relative fold of enrichment over IgGs. n(CAF strains)= 3, n(HDF strains)=3.

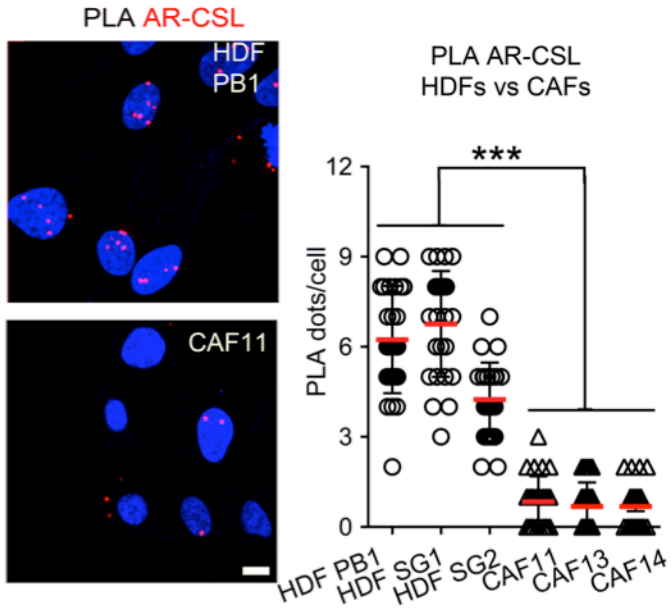

Supplemental Figure 10. AR-CSL association is reduced in CAFs.
(A) Proximity ligation assays (PLA) with antibodies against AR and CSL in three SCC derived CAFs and HDFs strains. Red fluorescence puncta resulting from the juxtaposition of anti-AR and anti-CSL antibodies were visualized by confocal microscopy with concomitant DAPI nuclear staining. Shown are representative images and quantification of the number of puncta per cell, as dots, and mean ± SD. Scale bar 10 μm. n(CAFs and HDFs strains) = 3 ***p<0.005 two-tailed unpaired t-test.

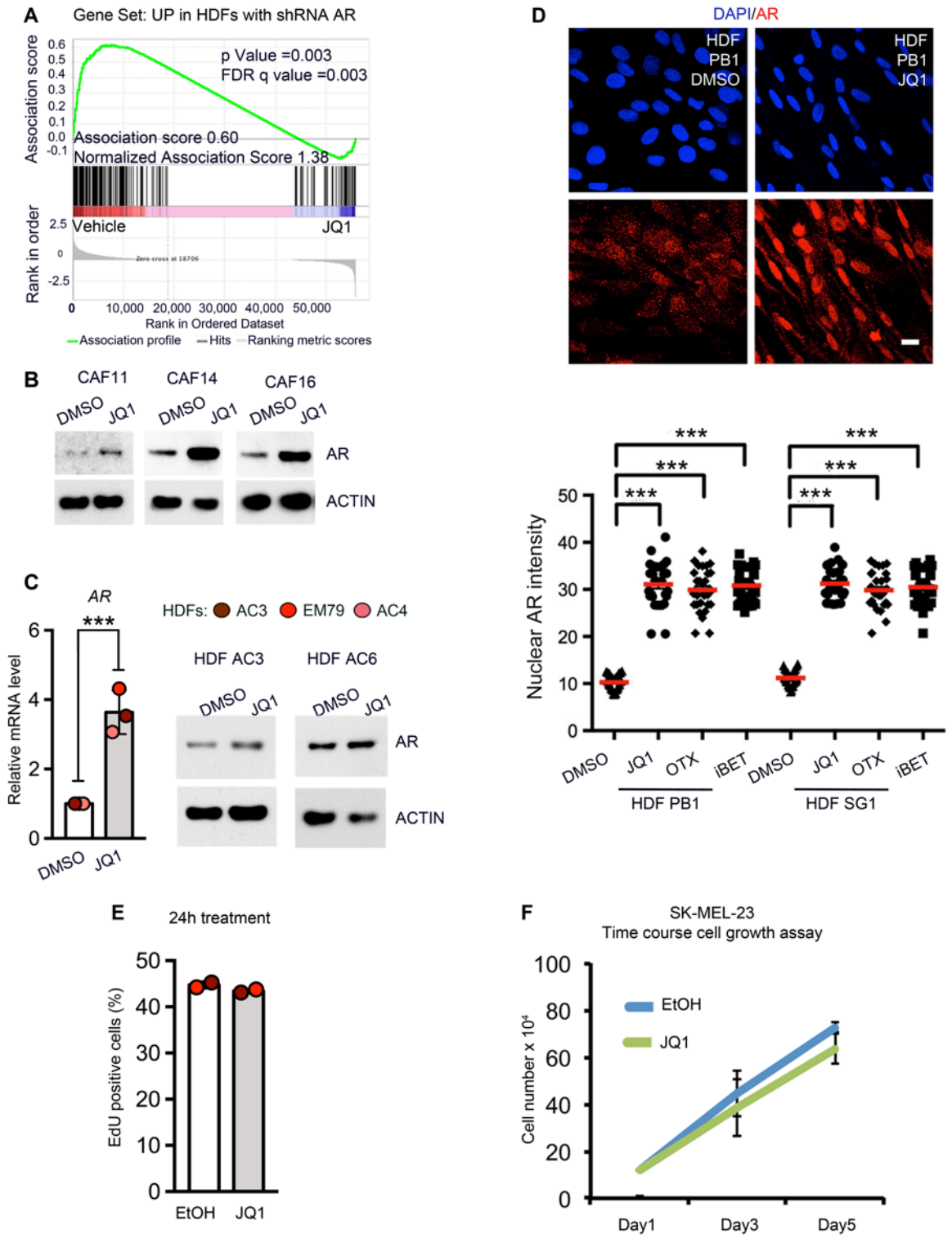

Supplemental Figure 11. Regulation of *AR* gene expression in HDFs by JQ1 treatment.
(A) GSEA of RNA-seq expression profile of three CAF strains with and without JQ1 treatment (500 nM for 2 days) versus vehicle (DMSO) (6) with a signature of up-regulated genes by *AR* silencing in HDFs. See Supplemental Table 2.
(B) Immunoblot analysis of *AR* expression in 3 independent SCC derived CAF and matched HDF strains treated with JQ1 (100 nM) or DMSO vehicle alone for 24h.
(C) RT-qPCR and immunoblot analysis of *AR* expression in independent HDF strains treated with JQ1 (100 nM) or DMSO vehicle alone for 24h. n(HDF strains)=3,***p<0.005, two-tailed unpaired t-test.

(D) Representative immunofluorescence images and quantification of AR signal in two HDF strains treated with different BET inhibitors (JQ1, OTX, iBET, 100 nM each) versus DMSO vehicle alone for 24h. Scale bar 20 μm. AR signal intensity values for each individual cell are indicated with mean ± SD. n(cell measurements) = 35, ***p<0.005, one-way ANOVA with Dunnett's test.
(E) EdU labeling assays of SK-MEL23 treated with JQ1 100 nM for 24h versus vehicle (ETOH). Data values for each experiment are represented as dots and mean ± SD. n(experiments) = 2.
(F) Growth curve of SK-MEL-23 treated with JQ1 100 nM for 24h versus vehicle (ETOH) plating an equal number of cell. Data are expressed as mean ± SD. n(experiments) = 2.

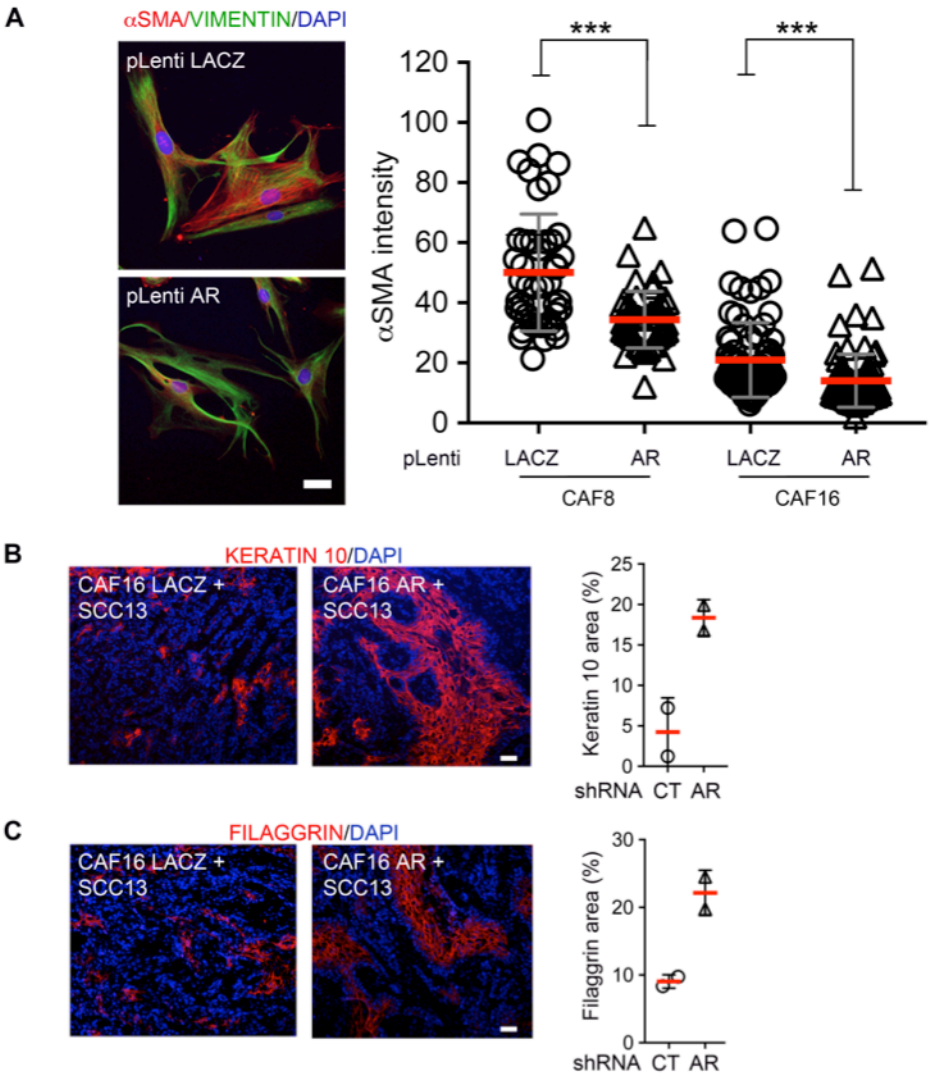

Supplemental Figure 12. AR over-expression restrains CAF activation and SCC tumor formation.

(A) Double immunofluorescence analysis of α-SMA (red) expression, with VIMENTIN as counterstaining (green), in two different CAFs strains plus/minus lentivirus-mediated *AR* overexpression. Shown are representative images with quantification of α-SMA signal intensity with values for each individual cell indicated as dots and mean as red lines. Values for each individual cell are indicated as dots with mean ± SD. n(cell measurements per condition) = 44,***p<0.005, two-tailed paired t-test. Scale bar 60 μm.

(B,C) Immunofluorescence analysis and quantification of Keratin 10 (B) and filaggrin (C) squamous differentiation markers in lesions formed by SCC13 cells admixed with CAF16 plus/minus AR over-expression. Shown are representative images and quantification for 2 tumor pairs, examining at least 4 independent field per lesion. Scale bar 60μm. Data are represented as mean ±SD. n(tumor pairs)=2.